First publ. in: Current Biology, Vol. 12, 2002, issue 21, pp. 1877-1884

Genetically Expressed Cameleon in *Drosophila melanogaster* Is Used to Visualize Olfactory Information in Projection Neurons

André Fiala,[1,4] Thomas Spall,[1] Sören Diegelmann,[1] Beate Eisermann,[2] Silke Sachse,[2] Jean-Marc Devaud,[3] Erich Buchner,[1] and C. Giovanni Galizia[2]

[1]Theodor-Boveri-Institut
Lehrstuhl für Genetik und Neurobiologie
Julius-Maximilians-Universität
Am Hubland
97074 Würzburg

[2]Institut für Neurobiologie
Freie Universität Berlin
Königin-Luise-Strasse 28-30
14195 Berlin
Germany

[3]Instituto Cajal
Consejo Superior de Investigaciones Cientificas
Madrid E-28002
Spain

Summary

Complex external stimuli such as odorants are believed to be internally represented in the brain by spatiotemporal activity patterns of extensive neuronal ensembles. These activity patterns can be recorded by optical imaging techniques. However, optical imaging with conventional fluorescence dyes usually does not allow for resolving the activity of biologically defined groups of neurons. Therefore, specifically targeting reporter molecules to neuron populations of common genetic identity is an important goal. We report the use of the genetically encoded calcium-sensitive fluorescence protein cameleon 2.1 [1] in the *Drosophila* brain. We visualized odorant-evoked intracellular calcium concentration changes in selectively labeled olfactory projection neurons both postsynaptically in the antennal lobe, the primary olfactory neuropil, and presynaptically in the mushroom body calyx, a structure involved in olfactory learning and memory. As a technical achievement, we show that calcium imaging with a genetically encoded fluorescence probe is feasible in a brain in vivo. This will allow one to combine *Drosophila's* advanced genetic tools with the physiological analysis of brain function. Moreover, we report for the first time optical imaging recordings in synaptic regions of the *Drosophila* mushroom body calyx and antennal lobe. This provides an important step for the use of *Drosophila* as a model system in olfaction.

Results and Discussion

Selective Expression of Cameleon 2.1 in Olfactory Projection Neurons

In *Drosophila*, olfactory receptor neurons (RNs) located in the antennae and maxillary palps terminate within the paired antennal lobes' (AL) 43 glomeruli [2]. The mode of axonal convergence resembles the connectivity pattern of the vertebrate olfactory bulb, because, in both systems, each sensory neuron expressing a certain type of receptor protein targets only one or very few specific glomeruli [3, 4]. The antennal lobe output neurons (projection neurons, PNs, which correspond to the vertebrate mitral/tufted cells) also ramify within the AL in a genetically determined way [5]. This stereotypic organization generates odotopic maps in terms of differential and combinatorial glomerular activities [6]. Complex signal integration within the insect AL results not only from the high degree of convergence — in *Drosophila*, from ~1300 RNs to 150–200 PNs [5] — but also from lateral inhibitory networks that shape both spatial patterns and temporal synchrony of PN responses [7, 8]. PNs project in two tracts to the lateral protocerebrum. Most of those neurons also form en passent arborizations in the mushroom body calyx (CX).

In order to visualize the spatiotemporal odorant representation in PNs, we used the P{Gal4} enhancer trap line GH 146 [5, 9] to express the calcium sensor protein cameleon 2.1 [1] under the control of a UAS enhancer [10] in ~90 out of the ~150 PNs, as shown in the whole-mount preparation of Figure 1A. Cameleon 2.1 consists of an enhanced cyan fluorescent protein (ECFP) and an enhanced yellow fluorescent protein (EYFP), both fused to a calmodulin sequence and the calmodulin target peptide M13 [1, 11]. When excited at 440 nm wavelength, calcium influx induces a shift in the ratio of EYFP to ECFP emission as a result of a calcium-dependent conformational change that leads to fluorescence resonance energy transfer (FRET) from ECFP to EYFP. We used two CCD cameras to simultaneously record the fluorescence emissions of both ECFP and EYFP (Figure 1B). In vivo preparations of the fly permitted direct optical access to the brain via a window in the head capsule exposing either the AL or the CX but leaving the antennae untouched. In order to visualize the spatial representation of odorant-evoked calcium signals at the postsynaptic dendrites of PNs within the AL or at their presynaptic terminals in the mushroom body CX, we measured the FRET responses to the six different odorants benzaldehyde, ethylacetate, isoamyl acetate, octanol, butanol, and propionic acid. The solvent mineral oil and blank air served as controls.

Odorant-Evoked Calcium Signals in the Antennal Lobes

In the in vivo preparation, the AL morphology with its glomerular structures is easily recognizable due to the cameleon expression (Figure 2A). For better orientation, the approximate field of view is indicated in Figure 1A by a frame. Color-coded activity patterns from different individuals (Figure 2B) stimulated with an odorant led to calcium rise in structural elements of the size of individual glomeruli (~10–30 μm). Repeated stimulation with the same odorant revealed highly reproducible patterns

[4]Correspondence: afiala@biozentrum.uni-wuerzburg.de

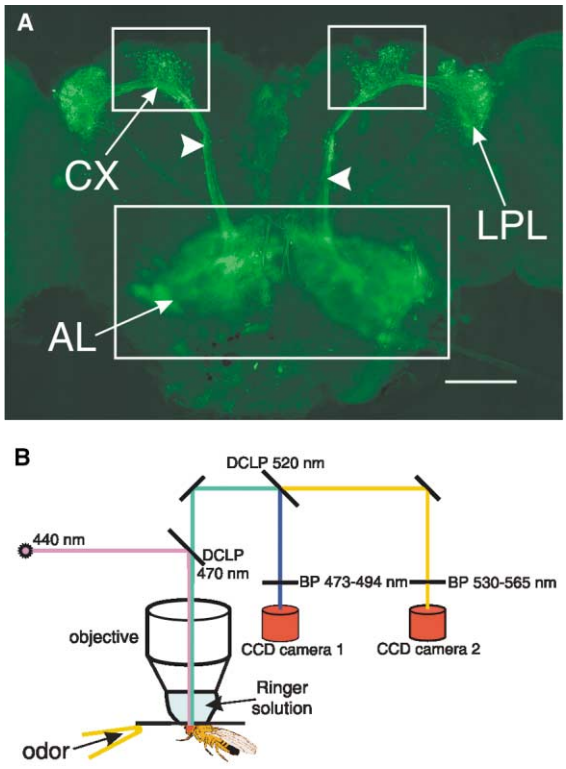

Figure 1. Cameleon Expression and Imaging Setup

(A) Whole-mount preparation of a *Drosophila* brain expressing cameleon 2.1 in projection neurons under the control of the Gal4 line GH 146. The image was taken with a color CCD camera (Axiocam, Zeiss) and was contrast enhanced with an unsharp mask filter (PhotoShop 5.5 program, Adobe). AL: antennal lobe, CX: calyx, LPL: lateral protocerebral lobe, arrowheads: inner antennocerebral tract. The scale bar represents 50 μm. Approximate areas imaged for the AL (see Figure 2) and the CX (see Figure 3) are indicated by boxes.
(B) Imaging setup for in vivo cameleon imaging. The 440 nm excitation is provided by a xenon lamp and a monochromator and is focused via a water immersion objective onto the brain. Emission wavelengths passing a 470 nm dichroic long pass mirror (DCLP 470 nm) are split up by a second dichroic long pass mirror (DCLP 520 nm), and the two beams are guided through band pass filters (BP 473–494 nm for the ECFP emission, and BP 530–565 nm for the EYFP emission). The two emissions are simultaneously recorded by two independent CCD cameras.

within any one animal. The combinatorial aspect of glomerular-like odorant representation is illustrated by the colored regions of activity superimposed onto the fluorescence pattern for different odorants (Figure 2B, right): different patterns of presumed glomeruli responded to different odorants in a partially overlapping manner. Although we could not morphologically identify the activated glomeruli, the similarity of spatial activity patterns observed for a given odorant in different individuals strongly supports that these patterns are also reproducible between individuals, similar to the situation in honeybees [12]. The observed variability between individuals reflects, at least to some extent, slight differences in orientation, which are also apparent when the left and right sides of the brain are compared (Figure 2B).

The temporal response profiles within the AL for three out of the six odorants and the mineral oil control are shown in Figure 2C for the two coordinates depicted in Figure 2A. Changes in intracellular calcium concentrations resulting in FRET are reflected by intensity changes of EYFP and ECFP emission in opposite directions. Motion and bleaching artifacts are characterized by changes in fluorescence intensity in the same direction. By calculating the ratio of EYFP/ECFP emissions, we thus obtain a clear indication of intracellular calcium concentration changes (black lines in Figure 2C). In a quantitative analysis of signal intensities evoked by the six odorants over the whole AL area ($n = 9–12$ animals, cf. the Experimental Procedures), we obtained a peak EYFP/ECFP ratio change of 1.23% ± 0.23% in response to the stimulus (mean ± SEM, $t = 5.4$, $p < 0.003$, t test). The calcium signals seen in our preparation were significantly smaller than those described for cell cultures [1] with an almost 1.5-fold increase in ratio emission. This was to be expected because, besides light scattering effects of the brain tissue, only a fraction of the labeled neurons respond to a certain odorant stimulus in a spatially very restricted way. Moreover, physiological stimuli such as odorants evoke calcium activities of smaller magnitudes than a stimulation with transmitters or drugs that may drive the calcium sensor into satiation. When the brain was flooded with ~10 mM KCl, causing neuronal depolarization, we observed an increase in the EYFP/ECFP ratio throughout the labeled structures of up to ~5%.

Maximum ratio changes in the various response patterns for the different odorants within the whole AL area were not significantly different. Thus, the different patterns evoked by different odorants cannot be ascribed only to different overall activity intensities. These differences in the spatial activity patterns for different odorants (Figure 2B) are also reflected in the time course of signal intensities (Figure 2C): the amplitudes of odorant-evoked signals at certain image coordinates are dependent on the particular stimulus. In the three examples shown in Figure 2, benzaldehyde induces weak signals at both selected coordinates, isoamylacetate gives a very strong signal at coordinate 2 and a weaker response at coordinate 1, and octanol leads to a strong response at coordinate 1 and a weaker response at coordinate 2. Mineral oil does not induce a response.

By adjusting a threshold, the response patterns can be more clearly visualized in the image's time series shown in Figure 2D, with false-color-coded suprathreshold signals superimposed onto the morphological fluorescence image. In general, the calcium signal outlasted the 1 s odorant stimulus (red bar). The onset of detectable signals was usually delayed compared to the stimulus, with a peak activity at ~0.5 s after the stimulus offset, i.e., ~1.5 s after stimulus onset. A direct comparison with earlier data generated by using ^{3}[H]2-deoxyglucose autoradiography [13] is not possible due to essential differences in the technique.

Odorant-Evoked Calcium Signals in the Calyx

Whereas little functional information is available for the lateral protocerebrum, the mushroom body is known to be involved in olfactory learning and memory [14–16]. To test if and how different odorants are spatially represented as neuronal activity within the dense ramifications of the mushroom body CX, we focused on one

CX; in some preparations, we successively focused on the two calyces of the fly. Again, a morphology image is given in Figure 3A, showing the cameleon fluorescence of PN axons forming the inner antennocerebral tract with their side branches arborizing in the CX (compare with the marked area in Figure 1A). The response patterns to different odorants were clearly spatially organized, with discrete areas of activity distributed over the calyx area (Figure 3B). In contrast to the AL (Figure 2B), the three images for each odorant were taken from three stimulations in the same fly. The reproducibility of the different patterns strongly suggests that odorant representations within the calyx are spatially specific. The angle of view differs between preparations, precluding comparisons of spatial activity patterns between animals.

The presynaptic arborizations of the PNs in the CX responded with a shorter delay compared to the postsynaptic dendrites in the AL (Figure 3C). In most CX recordings, the Ca^{2+} signals started immediately after the stimulus onset. This reflects the different roles played by calcium in these two compartments, i.e., synaptic vesicle release in the CX and postsynaptic integration in the AL. The EYFP/ECFP ratio changes (0.6% $\pm$ 0.06% mean $\pm$ SEM, n = 6 odorants, 1–5 averaged stimulations with each odorant in 10 animals, cf. the Experimental Procedures) measured over the whole CX area were smaller than the responses in the AL but were highly significant ($p < 0.0002$, n = 6, t = 9.7, t test). As in the AL, maximum ratio changes in the various response patterns measured over the whole CX area were not significantly different for the various odorants.

Interestingly, the combinatorial aspect of olfactory coding can be seen in the CX as well: whereas benzaldehyde elicits strong activity at both coordinate points, isoamylacetate activates only at coordinate 1. Octanol shows activation at both coordinates, but to a lower degree than benzaldehyde, and mineral oil does not lead to a detectable response. Averages of the three traces obtained in the same fly illustrate the reproducibility of the recordings (Figure 3D). Due to the smaller signals, bleaching effects are more pronounced in the CX compared to the AL, and this is most likely due to the fact that much smaller structures are exposed with higher magnification to similar total excitation energy. The predominant negative slope is apparently caused by more rapid bleaching of EYFP to ECFP. Superimposed on this are odorant responses correlating with the stimulus and random fluctuations, mainly due to motion. Figure 4 shows the images of suprathreshold activities superimposed onto the morphological image, visualizing the spatial activation of distinct regions by different odorants. Again, the calcium signal increases with little delay after stimulus onset and reaches its peak during or just after the 1 s stimulus (red bar).

We demonstrate that odorants evoke spatially restricted, odorant-specific domains of activity that appear to emerge and disappear in a monotonic fashion rather than, for example, complex activity waves that evolve in time. In that sense, odorant stimuli are represented in the CX in a mode similar to the AL, despite the different anatomical organization of the two brain regions. No such prominent, highly ordered structures, such as glomeruli in the AL, are apparent in the CX with its dense wiring. Electron microscopy studies show large presynaptic boutons of PN terminals surrounded by postsynaptic processes of Kenyon cells and inhibitory synapses of other neurons [17]. Since the spots of activity we observed are within the range of 5 $\pm$ 2 μm (20 randomly depicted activity spots) of the size that has been described for the presynaptic boutons [17], these microglomeruli could perhaps underlie our activity patterns. The olfactory glomerular activity pattern in the AL might therefore be mapped onto the mushroom body in a yet unknown rearrangement that results in discrete regions of input activity to Kenyon cells. This is in accordance with anatomical studies showing that projection neurons form stereotyped and spatially defined arborizations in the lateral protocerebrum and possibly, with a higher degree of interindividual variability, in the CX [18, 19]. The imaging technique described here will be useful to compare RN and PN activity patterns and to analyze odorant representations in the LPL.

A serious problem under in vivo conditions is small displacements of the brain due to hemolymph pumping and muscular contractions. We restricted muscle movements in the CX preparation by applying philanthotoxin, a blocker of muscular glutamate receptors that has been used in various insect preparations to block neuromuscular transmission [20, 21]. The effects of philanthotoxin on acetylcholine receptors have also been described [22] and cannot be excluded in our preparation. This drug significantly reduced brain movements but did not eliminate them completely. Using FRET-based sensors, opposite intensity changes resulting from the two emissions can be attributed to the physiological response, which thus can be discriminated from the syndirectional changes caused by motion artifacts. An improved version of cameleon with a higher signal-to-noise ratio has been reported recently [23]. Alternatively, calcium probes based on a single circularly permuted fluorescent protein have been shown to give much stronger signals [24–26] and will be tested under comparable conditions.

So far, functional imaging in the *Drosophila* brain with calcium-sensitive dyes has been limited to a superficial layer of mushroom body Kenyon cell somata [27]. Going a step further in complexity, Rosay et al. [28] expressed the Ca^{2+}-sensitive luminescent protein aequorin in the mushroom bodies of the *Drosophila* brain kept alive in a culture dish, and they observed slow oscillatory activity of unknown function. In a semi-in vivo preparation, calcium influx could be recorded in pharyngeal nerves and muscles of *C. elegans* with cameleon 2.1 [29]. We report the first successful use of a genetically encoded fluorescent probe in the brain of an almost intact animal. This technique is a promising new tool and can possibly be used in other genetically tractable organisms, such as mice and zebrafish. Its combination with other genetic tools, e.g., selective blocking of specific neuronal circuits [30] or the use of mutants, opens a new, wide field for neurophysiological analysis.

Experimental Procedures

Generation of UAS: Cameleon 2.1 Flies

The construct for the previous cameleon version 2.0 [11] was obtained from Dr. Christoph Schuster, Tübingen, Germany. Transgenic

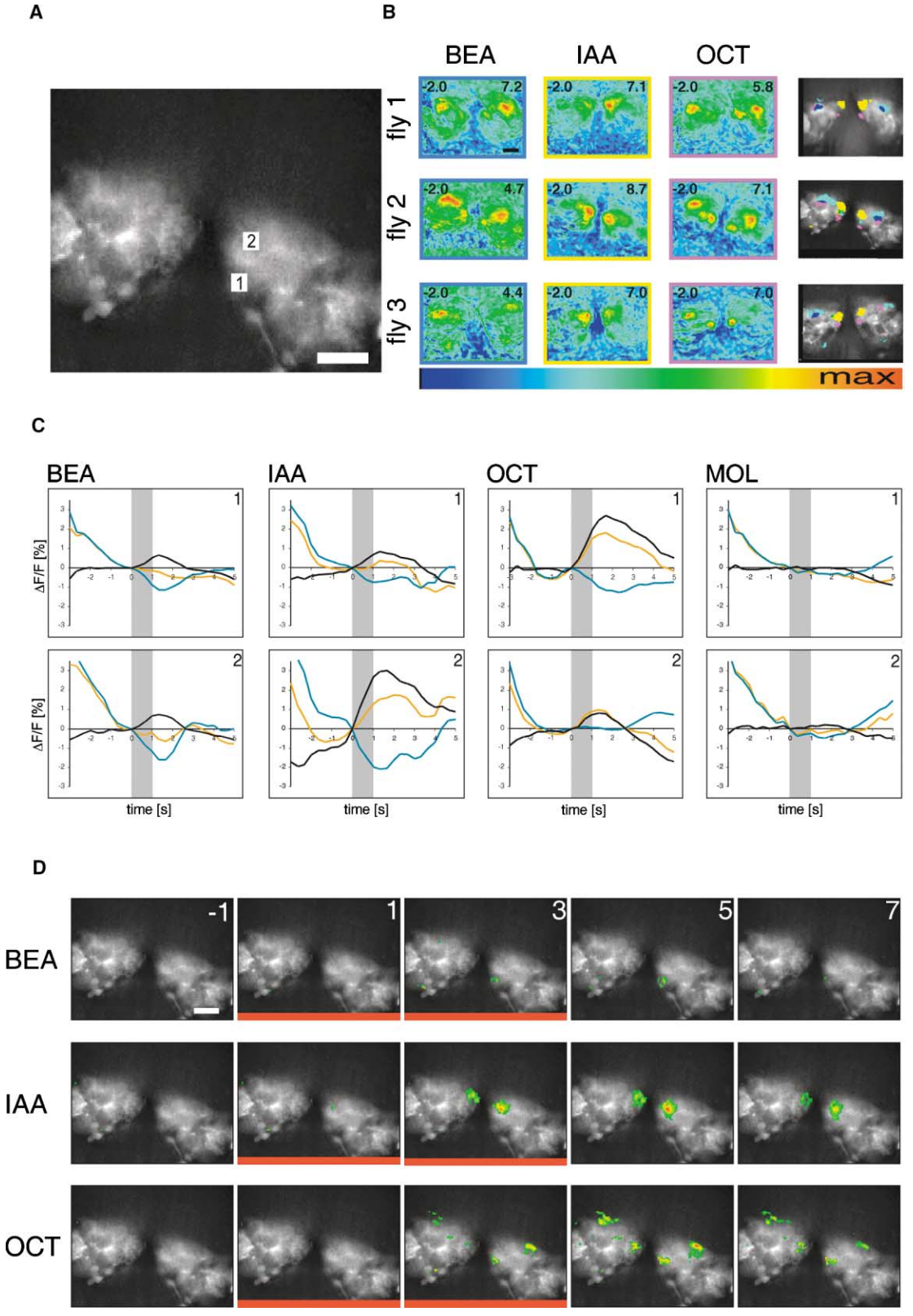

Figure 2. Odorant-Evoked Calcium Responses in the *Drosophila* Antennal Lobe

(A) Frontal view of the two ALs of one brain, as seen with EYFP fluorescence, after contrast enhancement. Compare this figure with Figure 1A for orientation and position of the area in the whole brain. The squares mark the positions evaluated in (C). This animal's position was slightly oblique; therefore, the symmetry line is not vertical. The scale bar represents 25 μm.

(B) Comparison of spatial FRET difference patterns between animals. Color-coded results from three different individuals for single stimulations

flies expressing cameleon 2.1 under UAS control were generated as described in [31]. For all experiments, the line UAS: cameleon 2.1-82 was chosen because of its strong expression [31]. Virgin females of the UAS line were crossed to male flies of the Gal4 line GH 146 [9] or vice versa to obtain offspring expressing cameleon 2.1 in projection neurons.

In Vivo Preparation of Flies

Flies that were 2–14 days old were immobilized on ice and were then fixed to a plexiglass stage. When recording from the ALs, flies were fixed at their neck, and the antennae were pulled forward with a fine metal wire. The head was covered with polyethylene foil, which was sealed against the cuticle with silicone. A hole was cut through the foil and cuticle, and this allowed optical access to the ALs. The brain was immediately bathed with Ringer solution (5 mM HEPES, 130 mM NaCl, 5 mM KCl, 2 mM $MgCl_2$, 2 mM $CaCl_2$, and 36 mM sucrose [pH 7.3]) [32], tracheal air sacks were removed from the head capsule, and the preparation was placed under the microscope. For CX measurements, a hole was stamped into a plastic coverslip and a thin transparency glued to it. Using dental glue (Protemp II, ESPE), the fly's head, thorax, and wings were fixed to the transparency with a minute needle between the head and thorax. The abdomen was fixed with a tiny drop of glue on the abdominal tip, and the legs were cut. A hole was cut through the transparency into the head capsule, with a drop of Ringer solution placed onto the opening. Tracheae and glands covering the brain were removed, and the fly was placed under the microscope. For CX measurements, 10 μl philanthotoxin (1 mM in Ringer solution) (Molecular Probes) was added to the Ringer above the brain to restrict muscle movements. Correlations between age and calcium signal intensities have not been investigated.

Imaging Setup

We used a modified imaging setup (TILL Photonics) consisting of a xenon lamp and a monochromator as light sources and two CCD cameras. The microscope (Olympus BX 50) was equipped with a 20 $\times$ W NA 0.5 objective for AL measurements and a 60$\times$ W NA 0.9 objective for CX recordings. Binning on chip was set to give a resolution of 1 μm/pixel for AL (image size 160 $\times$ 120 pixels, corresponding to 160 μm and 120 μm) and 0.66 μm/pixel for the CX (image size 80 $\times$ 60 pixels, corresponding 53 μm and 40 μm). Images were taken at a rate of 3 Hz. The excitation wavelength was 440 nm, and exposure times were 80–110 ms for AL and 160–220 ms for CX measurements. The primary dichroic mirror was 470 nm DCLP. Fluorescent light passing this dichroic was directed onto a 520 nm DCLP mirror followed by a 530–565 BP emission filter for EYFP and a 473–494 BP emission filter for ECFP.

Odorant Application

A constant air stream produced by an aquarium pump was guided through a Pasteur pipette with the tip placed at a distance of 5 mm from the fly's antennae. The pure odorants were diluted 1:100 in mineral oil. A total of 4 μl of this solution was placed on filter paper in a second Pasteur pipette laterally inserted into a hole in the first pipette. Using an electronic solenoid valve (Lee Company), odorant stimuli (1 s) were puffed into the constant air stream in an electronically controlled way. Odorant concentrations in the air stream or in front of the antennae have not been measured. Air flowrates were in the range of 1 ml/s. Individual flies were recorded for up to 2 hr, with interstimulus time intervals of about 2–5 min.

Data Analysis

Images were analyzed with custom-written IDL software (Research Systems). A total of 18 flies were measured for the AL, and 41 flies were measured for the CX. Flies were chosen for further analysis when they showed reliable calcium signals to odorants applied several times in a pseudorandomized manner. For the AL, 61 odorant stimulations in 9–12 flies were analyzed (in 3 flies, 1 or more odorants were missing); for the CX, 171 stimulations in 10 flies were analyzed. Images from the CCD cameras were median filtered to remove noise (size: 3 pixels) and were convoluted with a Mexican-hat function (diameter: 50 μm) to reduce scattered light effects. Then, the EYFP image was divided by the ECFP image. For traces, averages of a 3 $\times$ 3 pixel box are calculated as a function of time. Frames were numbered in relation to stimulus onset, with frame 0 starting with stimulus onset and prestimulus frames starting with negative numbers. Single-wavelength data are given as 100 $\times$ ΔF/F, where F is the mean for the prestimulus frames -4 to -2. Ratio data are 100 $\times$ (EYFP/ECFP). Traces were shifted to 0 at t = 0. For movies and individual frames, ratio images were convoluted with a 3 $\times$ 3 pixel box to reduce high-frequency noise. Odorant-evoked responses were calculated as the average of ratio frames 2–4 minus ratio frames -3 to -1. For quantification of EYFP/ECFP ratio signals, the maximum ratio signals evoked in the AL or CX area were measured. Correction for drifts in the time course of the ratio signal was obtained by calculating the average of frames -3 to -1 minus the average of frames -8 to -6. This value was then subtracted from the average of frames 2–4 minus the average of frames -3 to -1.

Supplementary Material

Supplementary Material including additional images of activity patterns in the calyx from different flies and the time series images in Figures 2D and 4 in the form of movies is available at http://images.cellpress.com/supmat/supmatin.htm.

Acknowledgments

We are grateful to Roger Tsien for granting the use of the cameleon construct, to Christoph Schuster for providing flies carrying a UAS: cameleon 2.0 insert, and to Gertrud Heimbeck and Reinhard Stocker for providing the Gal4 line GH 146. We also thank Randolf Menzel, Troy Zars, Henrike Scholz, and Martin Heisenberg for helpful discussions on the manuscript and for support. We are most grateful to the anonymous reviewers who helped to improve the manuscript substantially. This work was supported by the Deutsche Forschungs-

per odorant for three different odorants are shown. To the right, areas with the strongest activity for each odorant are superimposed onto an EYFP fluorescence image providing a morphological view. Here, purple areas indicate responses to octanol (OCT), cyan areas indicate responses to benzaldehyde (BEA), and yellow areas indicate responses to isoamyl acetate (IAA). Areas responding both to BEA and IAA are green, and overlapping regions of OCT and BEA are blue. While the glomeruli could not unequivocally be identified from their morphology, the similarity of the activity patterns between animals suggests that homologous glomeruli are excited by the same odorant in different animals. In each image, false-color coding scales the responses between -2.0% EYFP/ECFP and the maximum, which is indicated in each image (e.g., 5.8 for the upper octanol).

(C) Time courses of the responses to the odorants BEA, IAA, OCT, and the control mineral oil (MOL) in fly 2 (single stimulation each). Two different glomeruli are evaluated; the upper row of graphs correspond to position 1 in (A), and the lower row of graphs correspond to position 2 in (A). For each glomerulus and odorant, the response is shown for the EYFP (yellow line) and the ECFP (blue line) signal (both as % ΔF/F). The EYFP/ECFP ratio change is shown as a black line (also as % ratio). All curves are shifted to baseline before odorant stimulus onset (t = 0 s). Odorant stimulation is indicated by the gray bar.

(D) Spatiotemporal response patterns, shown as a sequence of images from the AL. Adjacent images are 0.66 s apart, i.e., every second frame is shown. Frame numbers are indicated in the upper-right corner of each frame, with 0 denoting stimulus onset. Odorant stimulus is indicated by the red bar. Ratio values above 0 are false-color coded on top of the morphological view of the two ALs. Note the bilateral symmetry of the odorant-evoked signals, the spatial differences between OCT and IAA, and the very weak responses to BEA in this animal. See also the movies in the Supplementary Material available with this article online.

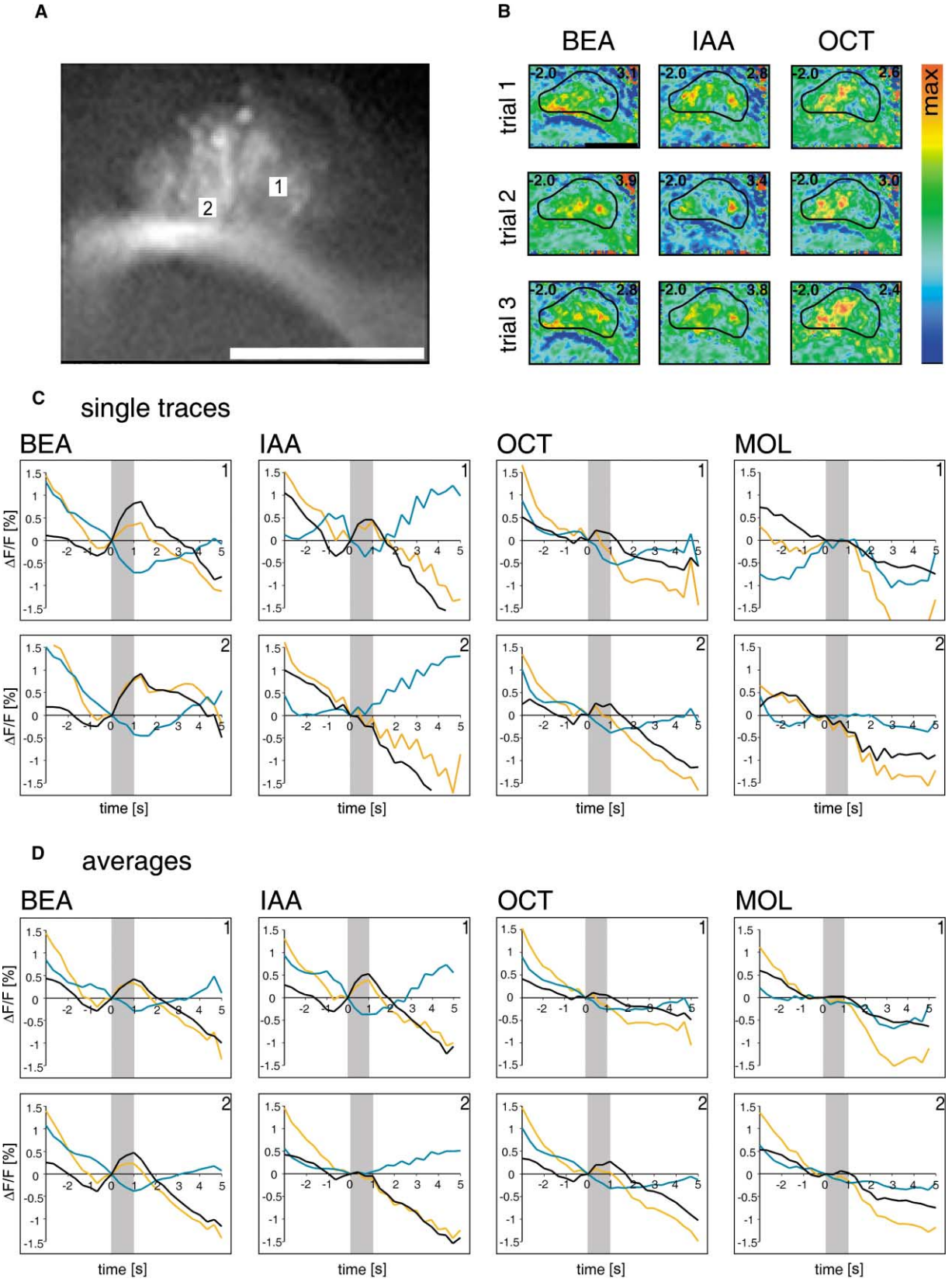

Figure 3. Odorant-Evoked Calcium Responses in the *Drosophila* Calyx

(A) A view onto one calyx, as seen with EYFP fluorescence and after contrast-enhancement, with the adjacent inner antennocerebral tract. The numbered squares mark the positions evaluated in (C). Compare this figure with Figure 1A for position of the area in the whole brain.

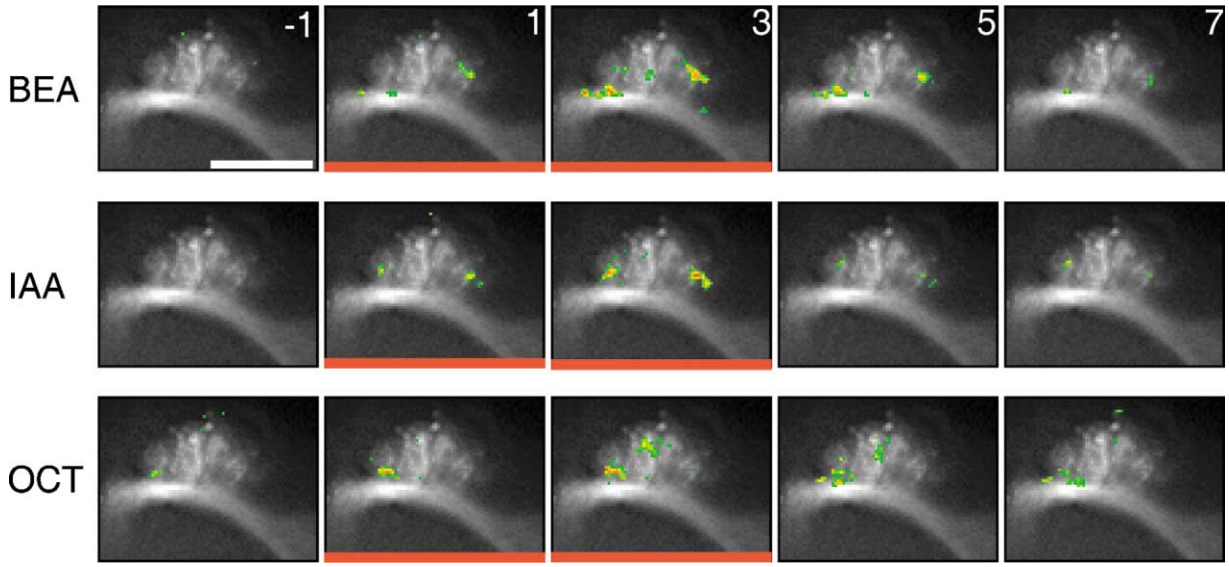

Figure 4. Spatiotemporal Response Patterns in the Calyx

Odorant-evoked response patterns, shown as a sequence of images from the calyx. Adjacent images are 0.66 s apart. The odorant stimulus is indicated by the red bar. Ratio values above 0 are false-color coded on top of the morphological view of the calyx. Note the spatial differences between BEA, OCT, and IAA. See also the movies in the Supplementary Material available with this article online. The scale bar represents 25 μm.

gemeinschaft (FI 821/1-1 and SFB 554/B2) and the Volkswagen Foundation (1/75 399).

Received: June 21, 2002
Revised: August 21, 2002
Accepted: August 22, 2002
Published: October 29, 2002

References

1. Miyawaki, A., Griesbeck, O., Heim, R., and Tsien, R.Y. (1999). Dynamic and quantitative Ca^{2+} measurements using improved cameleons. Proc. Natl. Acad. Sci. USA *96*, 2135–2140.
2. Laissue, P.P., Reiter, C., Hiesinger, P.R., Halter, S., Fischbach, K.F., and Stocker, R.F. (1999). Three-dimensional reconstruction of the antennal lobe in *Drosophila melanogaster*. J. Comp. Neurol. *405*, 543–552.
3. Vosshall, L.B., Wong, A.M., and Axel, R. (2000). An olfactory sensory map in the fly brain. Cell *102*, 147–159.
4. Mombaerts, P., Wang, F., Dulac, C., Chao, S.K., Nemes, A., Mendelsohn, M., Edmondson, J., and Axel, R. (1996). Visualizing an olfactory sensory map. Cell *87*, 675–686.
5. Jefferis, G.S., Marin, E.C., Stocker, R.F., and Luo, L. (2001). Target neuron prespecification in the olfactory map of *Drosophila*. Nature *414*, 204–208.
6. Galizia, C.G., and Menzel, R. (2001). The role of glomeruli in the neural representation of odours: results from optical recording studies. J. Insect Physiol. *47*, 115–129.
7. Sachse, S., and Galizia, C.G. (2002). Role of inhibition for temporal and spatial odor representation in olfactory output neurons: a calcium imaging study. J. Neurophysiol. *87*, 1106–1117.
8. Laurent, G., MacLeod, K., Stopfer, M., and Wehr, M. (1998). Spatiotemporal structure of olfactory inputs to the mushroom bodies. Learn. Mem. *5*, 124–132.
9. Stocker, R.F., Heimbeck, G., Gendre, N., and de Belle, J.S. (1997). Neuroblast ablation in *Drosophila* P[GAL4] lines reveals origins of olfactory interneurons. J. Neurobiol. *32*, 443–456.
10. Brand, A.H., and Perrimon, N. (1993). Targeted gene expression as a means of altering cell fates and generating dominant phenotypes. Development *118*, 401–415.
11. Miyawaki, A., Llopis, J., Heim, R., McCaffery, J.M., Adams, J.A., Ikura, M., and Tsien, R.Y. (1997). Fluorescent indicators for Ca^{2+} based on green fluorescent proteins and calmodulin. Nature *388*, 882–887.
12. Galizia, C.G., Sachse, S., Rappert, A., and Menzel, R. (1999). The glomerular code for odor representation is species specific in the honeybee *Apis mellifera*. Nat. Neurosci. *5*, 473–478.
13. Rodrigues, V. (1988). Spatial coding of lfactory information in the antennal lobes of *Drosophila melanogaster*. Brain Res. *453*, 299–307.
14. Heisenberg, M., Borst, A., Wagner, S., and Byers, D. (1985). Drosophila mushroom body mutants are deficient in olfactory learning. J. Neurogenet. *2*, 1–30.

The scale bar represents 25 μm.

(B) Comparison of spatial FRET difference patterns for repeated stimulation within one animal, with a single stimulation in each trial. Color-coded results for the three different odorants benzaldehyde (BEA), isoamyl acetate (IAA), and octanol (OCT) are shown. In each image, false-color coding scales the responses between −2.0 and the maximum, which is indicated in each image (e.g., 2.6 for the upper octanol). The outline of the CX is indicated by a black line.

(C) Time courses of the responses to single stimulations with BEA, OCT, IAA, and the control mineral oil (MOL). Two different coordinates are evaluated: coordinate 1 in (A) refers to the upper row, and coordinate 2 in (A) refers to the lower row. For each coordinate, the response is shown for the EYFP (yellow line) and the ECFP (blue line) signal (both as % $\Delta F/F$). The EYFP/ECFP ratio is shown as a black line (also as % ratio). All curves are shifted to baseline before odorant stimulus onset ($t = 0$ s). Odorant stimulation is indicated by the gray bar.

(D) Averages of the time courses of three responses to stimulations with BEA, OCT, IAA, and MOL. The same animal and coordinates that are shown in (C) are shown.

15. de Belle, J.S., and Heisenberg, M. (1994). Associative odor learning in *Drosophila* abolished by chemical ablation of mushroom bodies. Science *263*, 692–695.
16. Zars, T., Fischer, M., Schulz, R., and Heisenberg, M. (2000). Localization of a short-term memory in *Drosophila*. Science *288*, 672–675.
17. Yusuyama, K., Meinertzhagen, I.A., and Schürmann, F.W. (2002). Synaptic organization of the mushroom body calyx in *Drosophila melanogaster*. J. Comp. Neurol. *445*, 211–226.
18. Wong, A.M., Wang, J.W., and Axel, R. (2002). Spatial representation of the glomerular map in the *Drosophila* protocerebrum. Cell *109*, 229–241.
19. Marin, E.C., Jefferis, G.S.X.E., Komiyama, T., Zhu, H., and Luo, L. (2002). Representation of the glomerular olfactory map in the *Drosophila* brain. Cell *109*, 243–255.
20. Karst, H., Piek, T., Van Marle, J., Lind, A., and Van Weeren-Kramer, J. (1991). Structure-activity relationship of philanthotoxins –I. Pre- and postsynaptic inhibition of the locust neuromuscular transmission. Comp. Biochem. Physiol. C *98*, 471–477.
21. Benson, J.A., Schürmann, F., Kaufmann, L., Gsell, L., and Piek, T. (1992). Inhibition of dipteran larval neuromuscular synaptic transmission by analogues of philanthotoxin-4.3.3: a structure-activity study. Comp. Biochem. Physiol. *102C*, 267–272.
22. Nakanishi, K., Huang, X., Jiang, H., Liu, Y., Fang, K., Huang, D., Choi, S.K., Katz, E., and Eldefrawi, M. (1997). Structure-binding relation of philanthotoxins from nicotinic acetylcholine receptor binding assay. Bioorg. Med. Chem. *5*, 1969–1988.
23. Truong, K., Sawano, A., Mizuno, H., Hama, H., Tong, K.I., Mal, T.K., Miyawaki, A., and Ikura, M. (2001). FRET-based in vivo Ca2+ imaging by a new calmodulin-GFP fusion molecule. Nat. Struct. Biol. *8*, 1069–1073.
24. Baird, G.S., Zacharias, D.A., and Tsien, R.Y. (1999). Circular permutation and receptor insertion within green fluorescent proteins. Proc. Natl. Acad. Sci. USA *96*, 11241–11246.
25. Nagai, T., Sawano, A., Park, E.S., and Miyawaki, A. (2001). Circularly permuted green fluorescent proteins engineered to sense Ca^{2+}. Proc. Natl. Acad. Sci. USA *98*, 3197–3202.
26. Nakai, J., Ohkura, M., and Imoto, K. (2001). A high signal-to-noise Ca^{2+} probe composed of a single green fluorescent protein. Nat. Biotechnol. *19*, 137–141.
27. Wang, Y., Wright, N.J., Guo, H., Xie, Z., Svoboda, K., Malinow, R., Smith, D.P., and Zhong, Y. (2001). Genetic manipulation of the odor-evoked distributed neural activity in the *Drosophila* mushroom body. Neuron *29*, 267–276.
28. Rosay, P., Armstrong, J.D., Wang, Z., and Kaiser, K. (2001). Synchronized neural activity in the *Drosophila* memory centers and its modulation by amnesiac. Neuron *30*, 759–770.
29. Kerr, R., Lev-Ram, V., Baird, G., Vincent, P., Tsien, R.Y., and Schafer, W.R. (2000). Optical imaging of calcium transients in neurons and pharyngeal muscle of *C. elegans*. Neuron *26*, 583–594.
30. Kitamoto, T. (2001). Conditional modification of behavior in *Drosophila* by targeted expression of a temperature-sensitive shibire allele in defined neurons. J. Neurobiol. *47*, 81–92.
31. Diegelmann, S., Fiala, A., Leibold, C., Spall, T., and Buchner, E. (2002). Transgenic flies expressing cameleon 2.1 under UAS control. Genesis *34*, 95–98.
32. Estes, P.S., Roos, J., van der Bliek, A., Kelly, R.B., Krishnan, K.S., and Ramaswami, M. (1996). Traffic of dynamin within individual *Drosophila* synaptic boutons relative to compartment-specific markers. J. Neurosci. *16*, 5443–5456.

Supplementary Material

Genetically Expressed Cameleon in *Drosophila melanogaster* Is Used to Visualize Olfactory Information in Projection Neurons

André Fiala, Thomas Spall, Sören Diegelmann, Beate Eisermann, Silke Sachse, Jean-Marc Devaud, Erich Buchner, and C. Giovanni Galizia

Movies 1–3. Odorant-Evoked Spatiotemporal Activity Patterns in the Antennal Lobes

The movies represent the recordings shown as a time series of images in Figure 2D. Images were taken at a rate of 3 Hz and were converted into movies. Ratio values above 0 are false-color coded on top of the morphological view of the two ALs. The odorant stimulus is indicated by the red square appearing in the upper-left corner. Real time is indicated above the movies (s), with t = 0 s at odorant onset. EYFP/ECFP ratio values above 0 are false-color coded on top of the morphological view of the two ALs. Movie 1 shows the response to benzaldehyde, Movie 2 shows the response to isoamylacetate, and Movie 3 shows the response to octanol.

Movies 4–6. Odorant-Evoked Spatiotemporal Activity Patterns in the Calyx

The movies represent the recordings shown as a time series of images in Figure 4. Images were taken at a rate of 3 Hz and were converted into movies. Ratio values above 0 are false-color coded on top of the morphological view of the CX. The odorant stimulus is indicated by the red square appearing in the upper-left corner. Real time is indicated above the movies (s), with t = 0 s at odorant onset. EYFP/ECFP ratio values above 0 are false-color coded on top of the morphological view of the CX. Movie 4 shows the response to benzaldehyde, Movie 5 shows the response to isoamylacetate, and Movie 6 shows the response to octanol.

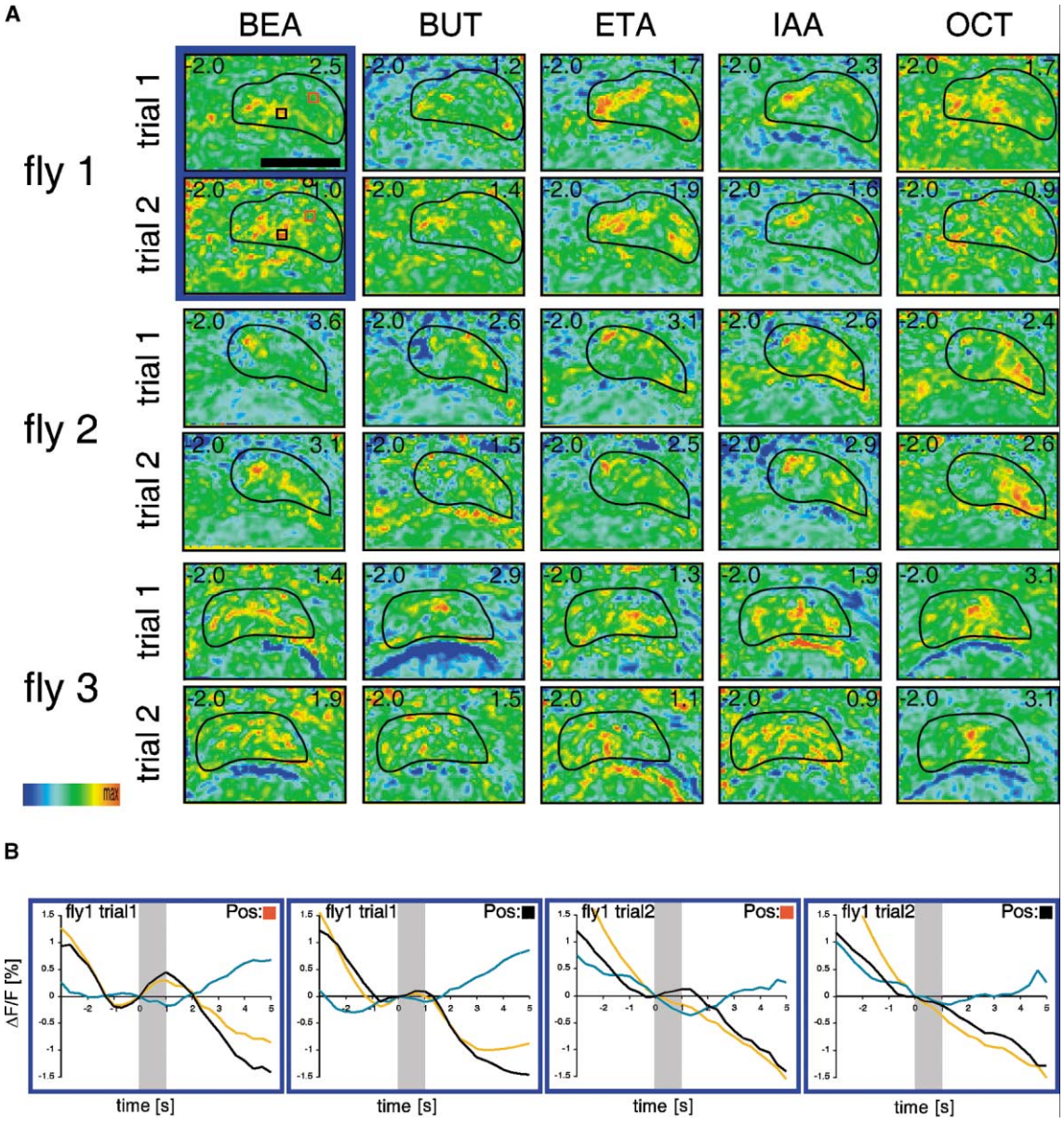

Figure S1. Odorant-Evoked Calcium Responses in the *Drosophila* Calyx of Three Different Flies

(A) Comparison of spatial FRET difference patterns for odorant stimulation within three animals, with two trials (single stimulation each). Color-coded results for the five different odorants benzaldehyde (BEA), butanol (BUT), ethyl acetate (ETA), isoamyl acetate (IAA), and octanol (OCT) are shown. In each image, false-color coding scales the responses between −2.0 and the maximum, which is indicated in each image (e.g., 1.7 for the upper octanol). The outline of the CX is indicated by a black line. The scale bar represents 25 μm. Note that repeated stimulation evokes similar patterns in any one fly for a given odorant. Signal peaks outside the CX region mainly represent activity in the adjacent antennocerebral tract or the proximal part of the lateral protocerebrum. Slight brain movements may also affect background signals. Between-animal comparisons are not possible due to spatial differences among different preparations.

(B) Time courses of the responses to two stimulations with BEA for one fly, indicated by the blue frame in (A). Two different coordinates are evaluated and are indicated by the red and black square in (A). For each coordinate, the response is shown for the EYFP (yellow line) and the ECFP (blue line) signal (both as % ΔF/F). The EYFP/ECFP ratio is shown as a black line (also as % ratio). All curves are shifted to baseline before odorant stimulus onset (t = 0 s). Odorant stimulation is indicated by the gray bar. Note that the signal amplitude for the two coordinates is slightly smaller at the second stimulation compared to the first one, showing that bleaching affects the signal intensity.